GPX4 and *GPX7* over-expression in human hepatocellular carcinoma tissues

E. Guerriero,[1] F. Capone,[1] M. Accardo,[2] A. Sorice,[1] M. Costantini,[3] G. Colonna,[4] G. Castello,[1] S. Costantini[1]

[1]Centro Ricerche Oncologiche di Mercogliano, Istituto Nazionale Tumori "Fondazione Giovanni Pascale", IRCCS, Napoli
[2]Sezione di Salute Mentale e Fisica, Sezione di Anatomia Patologica, Seconda Università degli Studi di Napoli
[3]Dipartimento di Biologia ed Evoluzione Organismi Marini, Stazione Zoologica Anton Dohrn, Villa Comunale, Napoli
[4]Servizio di Informatica Medica, Azienda Ospedaliera Universitaria, Seconda Università degli Studi di Napoli, Italy

Abstract

Hepatocellular carcinoma (HCC) is the most common type of liver cancer and is still one of the most fatal cancers. Hence, it needs to identify always new putative markers to improve its diagnosis and prognosis. The selenium is an essential trace mineral implicated as a key factor in the early stage of cancer and exerts its biological function through the selenoproteins. In the last years our group has been studying the involvement of some selenoproteins in HCC. However, no many data are reported in literature about the correlation between HCC and the glutathione peroxidases (GPXs), both selenium and non selenium-containing GPXs.

In this paper we have evaluated the *GPX4* and *GPX7* expression in some paraffin-embedded tissues from liver biopsy of patients with hepatitis C virus (HCV)-related cirrhosis and HCC by immunohistochemistry and RT-qPCR analysis. Our results evidenced that i) *GPX4* and *GPX7* had a statistically significant over-expression in HCC tissues compared to cirrhotic counterparts used as non tumor tissues, and ii) their expression was higher in grade III HCC tissues with respect to grade I-II samples. Therefore, we propose to use *GPX4* and *GPX7* as possible markers for improving HCC diagnosis/prognosis.

Introduction

Liver cancer is the second-leading cause of cancer mortality worldwide, accounting for approximately 600,000 cancer-related deaths annually.[1] Hepatocellular carcinoma (HCC), the most common type of liver cancer, generally develops from chronic liver injury,[2] and its risk factors are multiple, such as hepatitis B (HBV) or C virus (HCV) infection, alcohol-induced liver disease (ALD), nonalcoholic fatty liver disease (NAFLD), primary biliary cirrhosis, exposure to environmental carcinogens (particularly aflatoxin), or even type 2 diabetes and obesity.[3] Despite recent advances in diagnosis and management, the median survival of HCC patients is less than 8 months, and the disease is still one of the most fatal cancers.[4] Surgical resection, liver transplantation, and local ablation remain the only HCC curative modalities,[5,6] and recurrence occurs in up to 70% of patients within 5 years after resection.[7,8] Unfortunately, the molecular signaling mechanisms, which specifically lead to HCC, are shielded and perturbed by molecular signaling sustained by viral infection as well as other diseases such as, for instance, diabetes. Therefore, it is necessary to identify always new putative markers to improve the HCC prognosis. Recently some Authors evaluated the expression also of other two proteins, thymosin beta 4 (Tβ4) and thymosin beta 10 (Tβ10) in HCC tissues. This study showed the expression of both beta-thymosins in HCC with marked differences in their degree of expression and frequency of immunoreactivity. The higher incidence of Tβ10 expression and its higher reactivity in tumor cells involved in stromal invasion indicated a possible major role for Tβ10 in HCC progression.[9]

Some studies evidenced the role of selenium (Se) to assist cells in resisting to oxidative damage that is a major cause of cellular damage also because it was found implicated as a key factor in the early stage of cancer.[10] *In vivo*, Se is primarily present as selenoproteins to maintain the balance of the cellular redox state, and in humans there are 25 selenoproteins.[11] In the last years our group has been focusing on some selenoproteins and their involvement in HCC, also evaluating by immunohistochemistry (IHC) the expression of selenium binding protein-1 (SELENBP1), which is, *in vivo,* able to incorporate exogenously administered radioactive (75Se)-sodium selenite in the liver, as well as that of Selenoprotein M (SELM) in tissue samples of HCC patients.[12-14] These studies provided evidence that SELENBP-1, as well as selenium, is down-regulated in the liver tissue of HCC patients and that its gradual loss is associated with an increased malignant grade.[12,13] Moreover, we showed for the first time an increase of SELM expression in HCC liver tissues, and its correlation with their increased malignancy grade.[14] Also, we have recently carried out the analysis of the global expression of the seleno-transcriptome protein family in two human hepatocellular carcinoma cell lines (HepG2 and Huh7) compared to the normal human hepatocytes by means of the RT-qPCR analysis.[15,16] These studies have shown a signature of selenoprotein mRNAs specific for human hepatoma cells showing the genes that change their expression as a consequence of the liver cancer in the absence of any genetic mutations or viral infection, and, in particular, that in HepG2 and Huh7 cells there were three down-regulated and ten over-regulated genes, among which SELM, and two glutathione peroxidases such as *GPX4* and *GPX7*.[15,16]

In general, the GPXs belong to a family of phylogenetically related enzymes, and *GPX4* and *GPX7* are strictly correlated because the Cys-containing *GPX7* is evolved from a *GPX4*-like ancestor.[17] Actually, these two proteins present a percentage of sequence identity of about 50% and the same fold topology of an alpha-beta 3-layer sandwich type.[18] *GPX4* has some role in the regulation of apoptosis, whereas *GPX7* is reported to be involved in the protein folding.[17] Also, *GPX4* was found over-regulated at the protein level in human colon carcinoma tissue and the impaired expression of its gene in peripheral blood mononuclear cells was proposed as a biomarker of increased breast cancer risk.[19,20] Further, *GPX4* has been significantly associated with breast cancer survival among the patients with the highest Native American (NA) ancestry whereas its variants resulted to be correlated with the risk of lethal prostate cancer, and able to modify the relation between γ-tocopherol and prostate cancer survival.[21,22]

Recently, *GPX4* has been found to play an essential role in the hepatitis C virus (HCV)

Correspondence: Dr. Susan Costantini, Istituto Nazionale Tumori "Fondazione Giovanni Pascale", Cancer Research Center, Via Ammiraglio Bianco, 83013 Mercogliano (AV), Italy.
Tel. +39.0825.1911729 - Fax: +39.0825.1911705.
E-mail: s.costantini@isitutotumori.na.it

Key words: Hepatocellular carcinoma; *GPX4*; *GPX7*; immunohistochemistry; RT-qPCR.

Acknowledgments: the authors thank Marilina Russo for assistance in figure preparation.

Received for publication: 5 June 2015.
Accepted for publication: 7 October 2015.

European Journal of Histochemistry 2015; 59:2540
doi:10.4081/ejh.2015.2540

life cycle. In fact, the modulation of the oxidative stress, which specifically targets *GPX4* in chronic hepatitis C (CHC), may decrease the virions infectivity preventing the hepatocarcinogenesis, principally in patients who remain difficult to be treated in the new era of interferon-free regimens.[23] On the other hand, it is also reported that the dysfunction of *GPX7* in oesophageal cells increases the levels of reactive oxygen species (ROS) and oxidative DNA damage, which are common risk factors for Barrett oesophagus and oesophageal adenocarcinoma.[24] Hence, in this paper we report the evaluation of the *GPX4* and *GPX7* expression in tissue samples of patients with HCC by IHC and RT-qPCR analysis to understand if these two GPXs could be used as new markers for improving HCC diagnosis/prognosis.

Materials and Methods

Tissue sample

Paraffin-embedded HCC tissues obtained by biopsy from thirty patients were subjected to IHC and to reverse transcription-qPCR. In this study we used the cirrhotic counterparts of all tumor tissue sections as non tumor tissue controls. All patients in this study provided informed consent, and the study was approved by the Second University of Naples Ethics Committee. The clinic-pathological assessment of patients are listed in Table 1. In details, all patients had HCV-related cirrhosis and included 10 HCC with grade I, 11 HCC with grade II, and 9 HCC with grade III. No information related to follow-up data of these patients is known.

Table 1. Hepatocellular carcinoma patients clinical-pathological characteristics.

	Number of patients
Age	
≤70	14
≥70	16
Gender	
Female	13
Male	17
Grading	
I	10
II	11
III	9
Hepatitis C Virus (HCV) RNA	
Positive	30
Negative	None
Tumor size	
<2	6
2-5	16
>5	8

Tissue immunohistochemistry

Briefly, xylene dewaxed and alcohol rehydrated paraffin sections were placed in Coplin jars filled with a 0.01 M trisodium citrate solution and microwaved. After heating, slides were thoroughly rinsed in cool running water for 5 min. Sections were immersed in 3% H_2O_2 at room temperature for 30 min to block any endogenous peroxidase activity. They were then washed in Tris-buffered saline (TBS) pH 7.4 before incubating at 4°C overnight with rabbit anti-human polyclonal *GPX4* (LifeSpan BioSciences Inc., Seattle, WA, USA), diluted 10 µg/mL and with mouse anti-human monoclonal *GPX7* (LifeSpan BioSciences Inc), diluted 10 µg/mL. After incubation with the primary antibody, tissue sections were stained with species-specific biotinylated secondary antibodies, followed by peroxidase labelled streptavidine (Dako, Glostrup, Denmark); the signal was developed by using diaminobenzidine (DAB) chromogen (Dako) as substrate. Mayer's Hematoxylin solution was used as a nuclear counterstaining. Incubations with diluent antibody buffer omitting the specific antibody (for *GPX4* and *GPX7*) were used as negative controls (Supplementary Figure 1).

Scoring methods proposed by Sinicrope *et al*.[25] were utilised in the evaluation of immunoreactivity for both staining intensity and percentage positive of stained tumor cells. The percentage of positive cells that revealed stronger staining intensity in respect to the adjacent hepatocyte cells were scored as follows: 0 (if 0-4% of tumor cells were stained); 1 (if 5-25% of tumor cells were stained); 2 (if 26-50% of tumor cells were stained); 3 (if 51-75% of tumor cells were stained); and 4 (if more than 75% of tumor cells were stained). In order to determine the staining intensity, these categories were sub-classified as follows: 0, no expression, 1, extremely weak; 2, weak; 3, moderate; and 4, strong expression. Associations between immunohistochemical scores and clinicopathological characteristics of tissue specimens were evaluated by Pearson correlation coefficients and $P<0.05$ was considered statistically significant.

RNA preparation and RT-qPCR analysis

Total RNA was extracted from cirrhotic and tumoral liver FFPE (formalin-fixed paraffin embedded) tissue sections equivalent to 60 µm by RecoverAll Total Nucleic Acid Isolation Kit (Life Technologies-Ambion, Carlsbad, CA, USA) according to the manufacturer's instructions. The extracted RNA was dissolved in diethylpyrocarbonatetreated water, and its concentration and purity were assessed by measurement of optical density at 260/280 nm. RNA samples were quantified using a NanoDrop 2000 spectrophotometer (Thermo Scientific, Wilmington, DE). Two microgram of total RNA of each sample was reverse-transcribed with SuperScript VILO cDNA Synthesis kit (Life Technologies-Ambion) according to the manufacturer's instructions and subsequently diluted with nuclease-free water (Life Technologies-Ambion).

Sequences for mRNAs from the nucleotide data bank (National Center for Biotechnology Information, USA) were used to design primer pairs for RT-qPCR (Primer Express, Applied Biosystems, CA, USA). Oligonucleotides were obtained from Sigma Aldrich. The primer sequences are provided in Table 2. An appropriate region of 18S rRNA was used as control. RT-qPCR assays were run on an Step-One Real Time PCR System (Applied Biosystem). Two µL of cDNA were amplified in a total volume of 25 µL containing 2X SYBR Green PCR Master Mix (Applied Biosystem) and 300 nM of forward and reverse primers. The thermal cycling conditions were as follows: 5 min of denaturation at 95°C followed by 44 cycles of a two-step program (denaturation at 95°C for 30 sec and annealing/extension at 60°C for 1 min). For each target the primer sequences and the melting temperature are reported in Table 2. Dilutions of standards and test samples were run in duplicate. Each reaction was repeated at least three times. To show that only one PCR product has been formed using the designed *GPX4* and *GPX7* primers, we report as example four curves and the related separation of PCR products on a gel (Supplementary Figures 2

Table 2. Parameters for the RT-qPCR analysis.

Gene	Temperature (°C)	Sequence (5' -> 3')
GPX4	59.8	AGAGATCAAAGAGTTCGCCGC (21) TCTTCATCCACTTCCACAGCG (21)
GPX7	57.9	TTGGTCCCATCATTCTTGTGG (21) GGCTGGTGATTCACTGGTCAA (21) CTGCCCTATCAACTTTCGTG (20)
18S	60	GTAGTTTCTCAGGCTCCCTCTC (22)

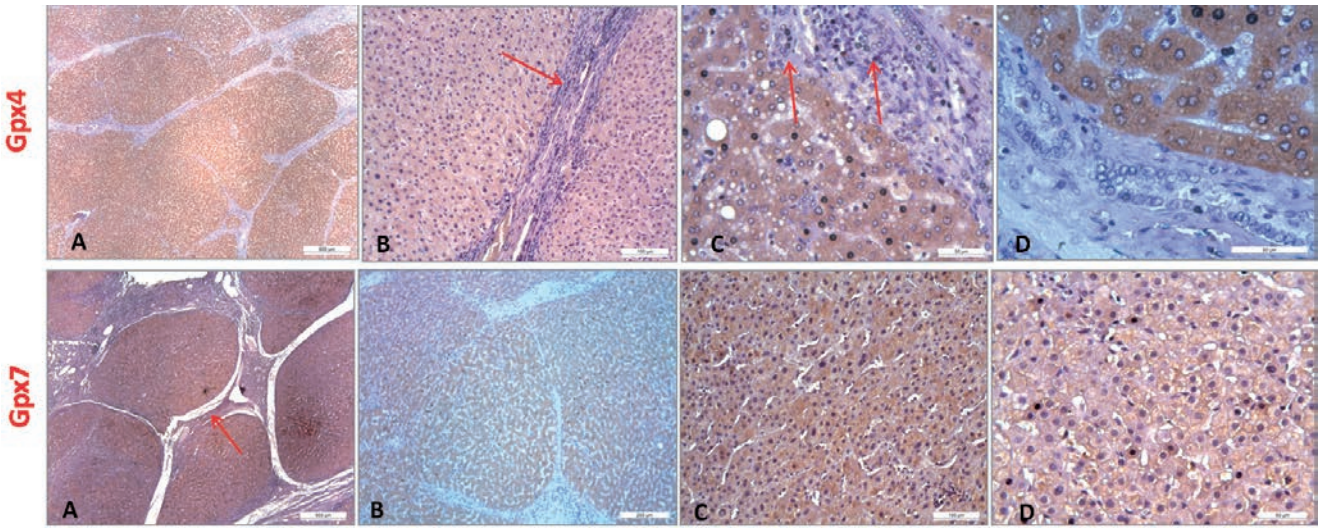

Figure 1. ***GPX4*** **and** ***GPX7*** **staining in cirrhotic tissues. The immunohistochemical observation of the human** ***GPX4*** **and** ***GPX7*** **expressions at 40x (A), 200x (B), 400x (C) and 630x (D) magnifications for** ***GPX4*** **and at 40x (A), 100x (B), 200x (C) and 400x magnifications for** ***GPX7*** **in cirrhotic tissues. In the** ***GPX4*** **staining it can be observed a portal lobule richly infiltrated by non-immunoreactive lymphocytic elements (B, red arrow), as well as bile ducts (C, red arrows) whose epithelia show no reactivity to this protein; more details were visible in panel D (630x). In the** ***GPX7*** **staining the hepatic parenchyma is organized into macronodular areas (A, red arrow), visible at higher magnification in the panel B (100x).**

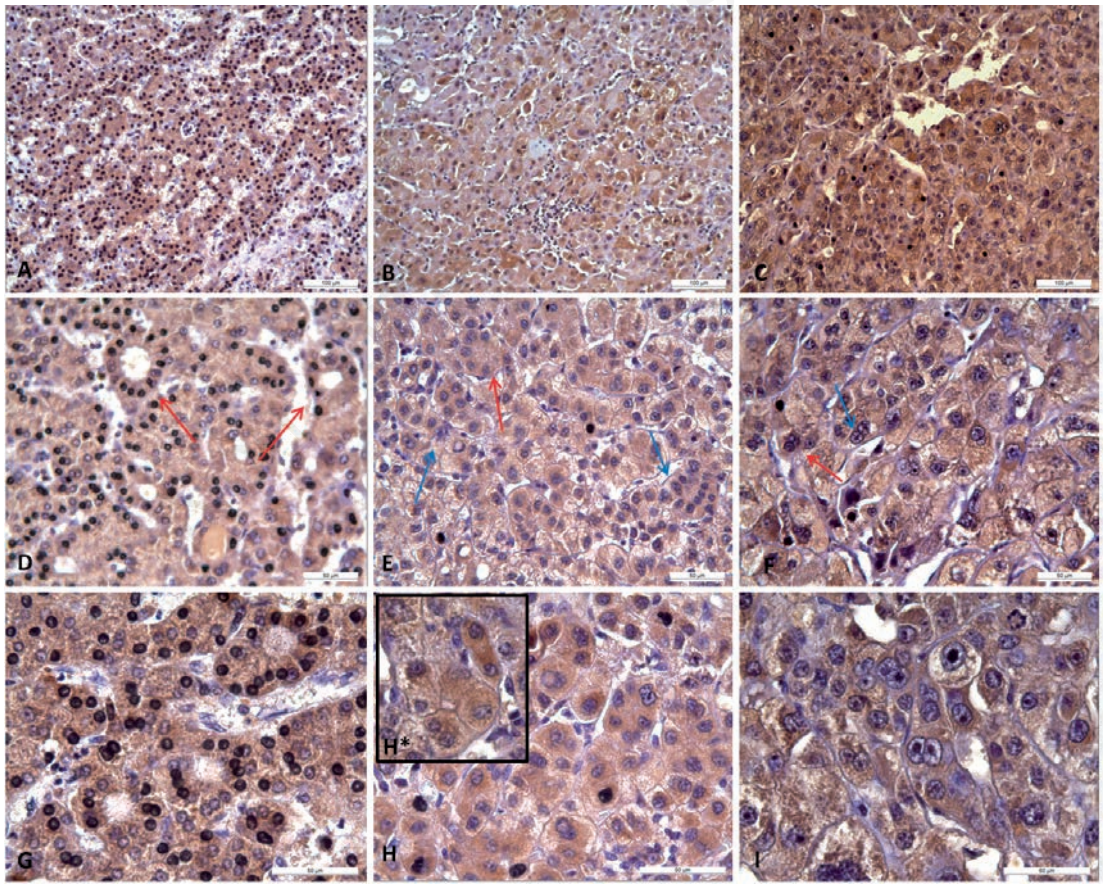

Figure 2. ***GPX4*** **staining. Immunohistochemical observation of the human** ***GPX4*** **expression in HCC tissues with grades I, II and III, respectively, at 200x (A, B, C), 400x (D, E, F) and 630x (G, H, box in H, I) magnifications. In particular, it was possible observe in HCC of grade I some acinar cell variants (D, red arrows, and higher magnification in G), in HCC of grade II (E, and higher magnification in H and box in H, respectively) a rosette-like structure (red arrow) and mono and bi-layered sheets (blue arrows), and in HCC of grade III (F, and higher magnification in I) a strong stain in highly undifferentiated (red arrow) and binuclear hepatocytes (blue arrow).**

and 3). Expression levels of each target gene in HCC tissue were compared with cirrhotic liver tissue. Data were normalized using the 18S rRNA as housekeeping gene which has been previously used in our recent paper.[15-16] The 2 x-fold change between expression levels in HCC and cirrhotic liver tissues was chosen as the threshold for significance of target genes. Statistical analyses (paired Student's *t*-test) were performed using Prism software (Graphpad Software, La Jolla, CA, USA). Significant differences in relative gene expression between HCC and cirrhotic liver tissue are marked by *(P<0.05), and ** (P<0.01).

Results and Discussion

GPX4 and *GPX7* expression in HCC tissues by immunohistochemistry

Collected tissues were subjected to *GPX4* and *GPX7* staining by IHC. *GPX4* staining in cirrhotic tissues showed a mild and specific cytoplasmic reactivity of the hepatocytes (Figure 1A). In Figure 1 B,C,D it has been possible to observe a portal lobule richly infiltrated by non-immunoreactive lymphocytic elements, and some bile ductules whose epithelia showed no reactivity to *GPX4*. In HCC tissues, the hepatocytes showed at 200x magnification a cytoplasmic positivity with stroma immunoreactivity and inflammatory elements interposed between the cirrhotic nodules as visible at 400x and 630 magnifications (Figure 2). In details, the cytoplasm of the hepatocytes showed a specific immunoreactivity for *GPX4*, gradually grown up from acinar cell variants in HCC tissues with a well-differentiated grade I (Figure 2D) to form a diffuse poorly differentiated grade III (Figure 2F). A diffuse positivity and a marked intensity of the cytoplasmic staining was observed in HCC samples with grade I, in a similar way to those with grade II (Figure 2 D,E). In particular, for the grade II HCC tissues we noted an asymmetrical arrangement of the hepatocytes, which are organized in rosette-like structures and in

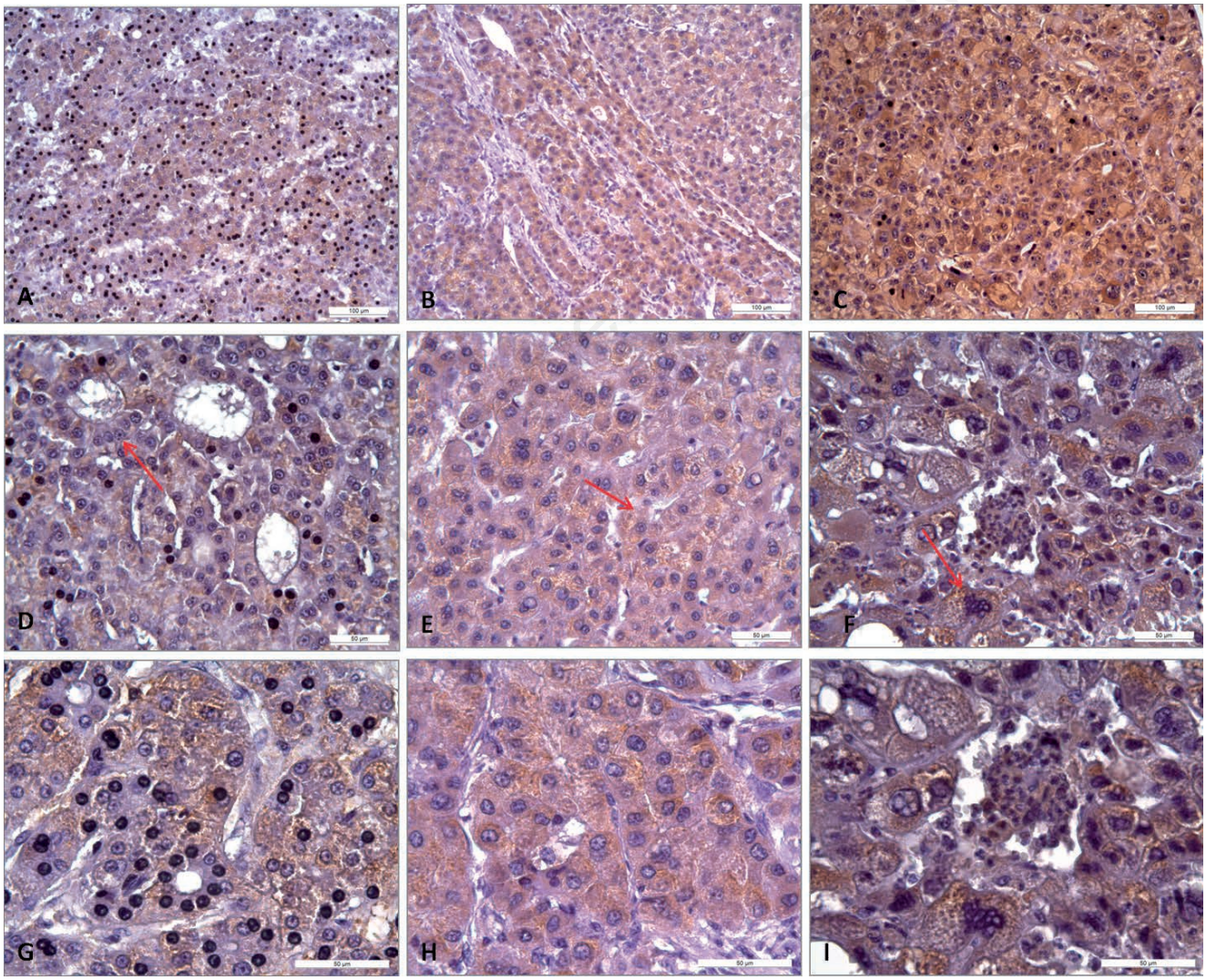

Figure 3. *GPX7* staining. Immunohistochemical at 200x (A, B, C) 400x (D, E, F) and 630x (G, H, I) magnifications. In particular, it was possible to observe in HCC of grade I acinar cell variant (D, red arrow, and higher magnification in G), in grade II HCC a multilayered sheet (E, red arrow, and higher magnification in H) and in grade III HCC atypical hepatocytes with monstrous nuclei (F, red arrow, and higher magnification in I).

mono and bi-layered sheets (Figure 2 E,H, and box in panel H). On the other hand, the HCC tissues with grade III showed a more intense cytoplasmic staining when compared to those with grades I and II. Moreover, the hepatocytes were distributed in multi-layered sheets and their greater cell volume was associated both to an increased nuclear polymorphism and to the presence of bi-nucleate hepatocytes (Figure 2 F,I). After *GPX7* staining in cirrhotic tissues, the hepatic parenchyma was organized into macro-nodular areas (Figure 1 A,B) and the hepatocytes expressed a mild cytoplasmic immuno-reactivity. *GPX7* showed a weak and diffuse immunoreactivity in grade I HCC tissues similarly to those with grade II whereas the staining became more widespread and intense in grade III HCC tissues (Figure 3). In grade I and II HCC tissues we observed *GPX7* plurifocal and moderate positivity (Figure 3A, 3 D,G,B,E,H). In particular, in grade II HCC tissues there was a strong architectural disorder with hepatocytes cellular distribution in multilayered sheets (Figure 3 E,H). In grade III HCC the hepatocytes were atypical with monstrous nuclei and prominent nucleoli of variable sizes (Figure 3 F,I).

These evaluations have suggested that the gradual raise of *GPX4* and *GPX7* expression were associated with an increased malignant grade. Actually, the cells percentage and the expression intensity increased from better differentiated histopathological forms to those poorly differentiated. In particular, using scoring methods proposed by Sinicrope *et al.*[25] for *GPX4* staining we can underline that: i) seven HCC tissue samples displayed a weak expression (with score 2); ii) fourteen revealed a moderate expression (score 3); and iii) nine evidenced a strong expression (score 4). For *GPX7* staining we can underline that: i) six HCC tissue samples displayed a weak expression (score 2); ii) sixteen revealed a moderate expression (score 3); and iii) eight evidenced a strong expression (score 4). A significant correlation was detected between the immunohistochemical scores and cancer progression/grading (P<0.05).

Analysis of *GPX4* and *GPX7* expression in HCC/cirrhotic tissues by RT-qPCR analysis

GPX4 and *GPX7* gene expression levels in human HCC tissues were evaluated by RT-qPCR compared to the cirrhotic liver tissue. No significant change in *GPX4* and *GPX7* expression levels between the grade I and grade II HCC samples was observed therefore we treat together their gene expression levels. In details, Figure 4 shows that: i) *GPX4* and *GPX7* had a statistically significant over-expression in HCC tissues; and ii) their expression was higher in grade III HCC tissues with respect to grade I-II samples. It highlighted that *GPX4* and *GPX7* expression was associated with an increased malignancy grade. However, these gene data agreed with the protein *GPX4* and *GPX7* over-expression obtained by IHC and with our gene data obtained on two HCC cell lines, HepG2 and Huh7, when compared to normal human hepatocyte cells.[16] Then, we evaluated the correlation coefficient between the *GPX4* and *GPX7* expression levels and the clinical-pathological data of HCC patients. A significant correlation was detected between the *GPX4* and *GPX7* gene expression levels and tumor grading (P=0.012 and P=0.043, respectively) whereas no correlation has been found between *GPX4* and *GPX7* expression and age/gender/tumor size.

In conclusion in this paper i) we evaluated the *GPX4* and *GPX7* expression in HCC tissue samples by IHC and RT-qPCR; ii) we verified that both these GPXs had a statistically significant over-expression; iii) this over-expression was associated with an increased malignancy grade. Furthermore, this paper highlighted for the first time that the *GPX4* and *GPX7* over-expression in human HCC tissues can be easily and precisely detected by the simple IHC or RT-qPCR techniques.

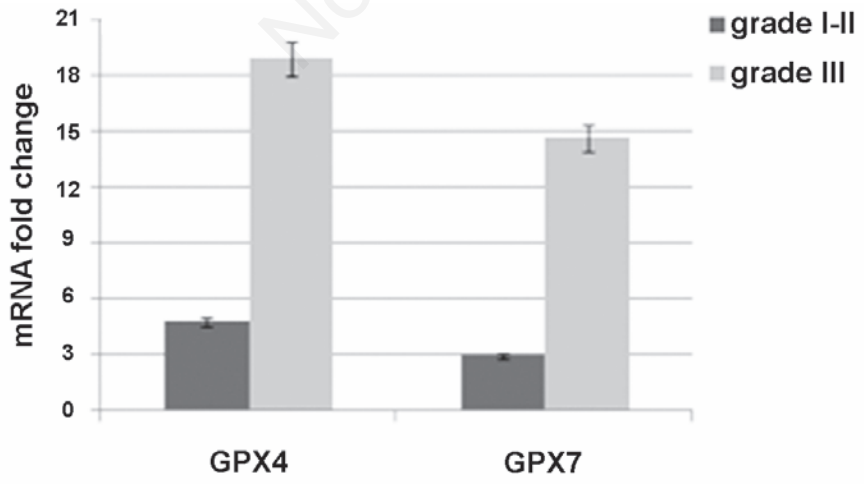

Figure 4. mRNA fold change evaluated between HCC tissues and cirrhotic liver tissues used as control for the expression levels of *GPX4* and *GPX7*.

References

1. International Agency for Research on Cancer. GLOBOCAN 2012: estimated cancer incidence, mortality and prevalence worldwide in 2012. International Agency for Research on Cancer, Lyon; 2013.
2. El-Serag HB, Rudolph KL. Hepatocellular carcinoma: epidemiology and molecular carcinogenesis. Gastroenterology 2007; 132:2557-76.
3. Costantini S, Capone F, Guerriero E, Marfella R, Sorice A, Maio P, et al. Cytokinome profile of patients with type 2 diabetes and/or chronic hepatitis C infection. PLoS One 2012;7:e39486.
4. El Serag HB. Hepatocellular carcinoma: recent trends in the United States. Gastroenterology 2004;127:S27-S34.
5. Bruix J, Llovet JM. Prognostic prediction and treatment strategy in hepatocellular carcinoma. Hepatology 2002;35:519-24.
6. Bruix J, Sherman M. Management of hepatocellular carcinoma. Hepatology 2005;42:1208-36.
7. Imamura H, Matsuyama Y, Tanaka E, Ohkubo T, Hasegawa K, Miyagawa S, et al. Risk factors contributing to early and late phase intrahepatic recurrence of hepatocellular carcinoma after hepatectomy. J Hepatol 2003;38:200-7.
8. Llovet JM, Fuster J, Bruix J. Intention-to-treat analysis of surgical treatment for early hepatocellular carcinoma: resection versus transplantation. Hepatology 1999; 30:1434-40.
9. Theunissen W, Fanni D, Nemolato S, Di Felice E, Cabras T, Gerosa C, et al. Thymosin beta 4 and thymosin beta 10 expression in hepatocellular carcinoma. Eur J Histochem 2014;58:2242.

10. Valko M, Rhodes CJ, Moncol J, Izakovic M, Mazur M. Free radicals, metals and antioxidants in oxidative stress-induced cancer. Chem Biol Interact 2006;160:1-40.
11. Bellinger FP, Raman AV, Reeves MA, Berry MJ. Regulation and function of selenoproteins in human disease. Biochem J 2009; 422:11-22.
12. Raucci R, Colonna G, Guerriero E, Capone F, Accardo M, Castello G, et al. Structural and functional studies of the human selenium binding protein-1 and its involvement in hepatocellular carcinoma. Biochim Biophys Acta 2011;1814:513-22.
13. Di Stasio M, Volpe MG, Colonna G, Nazzaro M, Polimeno M, Scala S, et al. A possible predictive marker of progression for hepatocellular carcinoma. Oncol Lett 2011;2: 1247-51.
14. Guerriero E, Accardo M, Capone F, Colonna G, Castello G, Costantini S. Assessment of the Selenoprotein M (SELM) over-expression on human hepatocellular carcinoma tissues by immunohistochemistry. Eur J Histochem 2014;58:2433.
15. Costantini S, Di Bernardo G, Cammarota M, Castello G, Colonna G. Gene expression signature of human HepG2 cell line. Gene 2013;518:335-345.
16. Guariniello S, Di Bernardo G, Colonna G, Cammarota M, Castello G, Costantini S. Evaluation of the selenotranscriptome expression in two hepatocellular carcinoma cell lines. Anal Cell Pathol (Amst) 2015;2015:419561.
17. Brigelius-Flohé R, Maiorino M. Glutathione peroxidases. Biochim Biophys Acta 2013;1830:3289-303.
18. Scheerer P, Borchert A, Krauss N, Wessner H, Gerth C, Höhne W, et al. Structural basis for catalytic activity and enzyme polymerization of phospholipid hydroperoxide glutathione peroxidase-4 (*GPX4*). Biochemistry 2007;46:9041-9.
19. Yagublu V, Arthur JR, Babayeva SN, Nicol F, Post S, Keese M. Expression of selenium-containing proteins in human colon carcinoma tissue. Anticancer Res 2011;31: 2693-8.
20. Bermano G, Smyth E, Goua M, Heys SD, Wahle KW. Impaired expression of glutathione peroxidase-4 gene in peripheral blood mononuclear cells: a biomarker of increased breast cancer risk. Cancer Biomark 2010;7:39-46.
21. Pellatt AJ, Wolff RK, John EM, Torres-Mejia G, Hines LM, Baumgartner KB, et al. SEPP1 influences breast cancer risk among women with greater native american ancestry: the breast cancer health disparities study. PLoS One 2013;8:e80554.
22. Van Blarigan EL, Ma J, Kenfield SA, Stampfer MJ, Sesso HD, Giovannucci EL, et al. Plasma antioxidants, genetic variation in SOD2, CAT, GPX1, *GPX4*, and prostate cancer survival. Cancer Epidemiol Biomarkers Prev 2014;23:1037-46.
23. Brault C, Lévy P, Duponchel S, Michelet M, Sallé A, Pécheur EI, et al. Glutathione peroxidase 4 is reversibly induced by HCV to control lipid peroxidation and to increase virion infectivity. Gut 2014;65:144-54.
24. Peng DF, Hu TL, Soutto M, Belkhiri A, El-Rifai W. Glutathione peroxidase 7 suppresses bile salt-induced expression of pro-inflammatory cytokines in Barrett's carcinogenesis. J Cancer 2014;5:510-7.
25. Sinicrope FA, Ruan SB, Cleary KR, Stephens LC, Lee JJ, Levin B. Bcl-2 and p53 oncoprotein expression during colorectal tumorigenesis. Cancer Res 1995; 55:237-41.